

# Observational constraints on Galileon cosmology

Savvas Nesseris,<sup>1</sup> Antonio De Felice,<sup>2</sup> and Shinji Tsujikawa<sup>2</sup>

<sup>1</sup>*The Niels Bohr International Academy and DISCOVERY Center,  
The Niels Bohr Institute, Blegdamsvej 17, DK-2100, Copenhagen Ø, Denmark\**

<sup>2</sup>*Department of Physics, Faculty of Science, Tokyo University of Science,  
1-3, Kagurazaka, Shinjuku-ku, Tokyo 162-8601, Japan†*

(Dated: October 29, 2018)

We study the cosmology of a covariant Galileon field  $\phi$  with five covariant Lagrangians and confront this theory with the most recent cosmological probes: the type Ia supernovae data (Constitution and Union2 sets), cosmic microwave background (WMAP7) and the baryon acoustic oscillations (SDSS7). In the Galileon cosmology with a late-time de Sitter attractor, there is a tracker that attracts solutions with different initial conditions to a common trajectory. Including the cosmic curvature  $K$ , we place observational constraints on two distinct cases: (i) the tracker, and (ii) the generic solutions to the equations of motion. We find that the tracker solution can be consistent with the individual observational data, but it is disfavored by the combined data analysis. The generic solutions fare quite well when a non-zero curvature parameter  $\Omega_K^{(0)}$  is taken into account, but the Akaike and Bayesian information criteria show that they are not particularly favored over the  $\Lambda$ CDM model.

## I. INTRODUCTION

The quest to distinguish between a cosmological constant and dynamical dark energy models has been one of the main topics in cosmology. The equation of state  $w_{\text{DE}}$  of dark energy can be constrained not only by the Supernovae Ia (SN Ia) data [1] but by the observations of Cosmic Microwave Background (CMB) [2] and Baryon Acoustic Oscillations (BAO) [3, 4]. For constant  $w_{\text{DE}}$  the combined data analysis of CMB+BAO+SN Ia by the WMAP group has given a tight constraint  $w_{\text{DE}} = -0.980 \pm 0.053$  (68 % confidence level) in the flat Universe [5]. However, the present observations still allow a large variation of the dark energy equation of state in terms of the redshift  $z$ . Moreover, inclusion of the cosmic curvature further weakens the constraints on  $w_{\text{DE}}(z)$ .

Over the past decade, many dynamical dark energy models have been proposed as an alternative to the cosmological constant (see Refs. [6] for review). They are broadly classified into two classes—(i) Modified matter models, and (ii) Modified gravity models. In the class (i) the accelerated expansion of the Universe is induced by a modified matter source, whereas in the class (ii) the large-distance modification of gravity gives rise to the cosmic acceleration. The representative model of the class (i) is quintessence based on a minimally coupled scalar field [7], but in general there is a degeneracy around  $w_{\text{DE}} = -1$  if we constrain the quintessence potential from observations.

The modified gravity models proposed so far consist of  $f(R)$  gravity [8], scalar-tensor theory [9], the Dvali-Gabadadze-Porrati (DGP) braneworld [10] model, the Gauss-Bonnet gravity [11],  $f(R, \mathcal{G})$  gravity [12], and so

on. In general we need to recover the General Relativistic behavior in the region of high density for the consistency with solar-system experiments [13], while the large-distance modification of gravity leads to the cosmic acceleration today. Moreover we require that the models are free from ghosts and instabilities [14]. For example, the DGP model is plagued by the ghost problem [15] in addition to the incompatibility with observational constraints [16]. The dark energy models in which the Lagrangian includes a general function  $f$  of the Gauss-Bonnet term  $\mathcal{G}$  also result in violent instabilities for small-scale perturbations [17]. In  $f(R)$  gravity and scalar-tensor theory, the functions  $f(R)$  or the field potentials need to be carefully designed to satisfy the above-mentioned demands [18].

In the DGP model a brane-bending mode  $\phi$  (i.e. longitudinal graviton) gives rise to a field self-interaction of the form  $\square\phi(\partial^\mu\phi\partial_\mu\phi)$  through the mixing with the transverse graviton [19]. This allows the decoupling of the field  $\phi$  from gravitational dynamics in the local region by the so-called Vainshtein mechanism [20]. Then the General Relativistic behavior can be recovered within a radius larger than the solar-system scale. The self-interaction  $\square\phi(\partial^\mu\phi\partial_\mu\phi)$  satisfies the Galilean symmetry  $\partial_\mu\phi \rightarrow \partial_\mu\phi + b_\mu$  in the flat space-time. While the DGP model suffers from the ghost problem, the extension of the field self-interaction to more general forms satisfying the Galilean symmetry may allow us to avoid the appearance of ghosts.

Nicolis *et al.* [21] showed that there are only five field Lagrangians  $\mathcal{L}_i$  ( $i = 1, \dots, 5$ ) that respect the Galilean symmetry in the Minkowski background. These terms lead to only the second-order field equations and hence we do not need to worry about extra degrees of freedom coming from higher-order derivatives.

If the Lagrangians  $\mathcal{L}_i$  are varied in the curved space-time, the terms  $\mathcal{L}_{4,5}$  give the field equations higher than the second-order. Deffayet *et al.* [22] derived the covariant Lagrangians  $\mathcal{L}_i$  ( $i = 1, \dots, 5$ ) that result in only

\*Electronic address: nesseris@nbi.dk

†Electronic address: defelice@rs.kagu.tus.ac.jp

the second-order equations, while recovering the Galilean symmetry in the Minkowski space-time. This can be achieved by introducing field-derivative couplings with the Ricci scalar  $R$  and the Einstein tensor  $G_{\nu\rho}$  in the expression of  $\mathcal{L}_{4,5}$ . Since the existence of those terms affects the effective gravitational coupling, the Galileon gravity based on the covariant Lagrangians  $\mathcal{L}_i$  ( $i = 1, \dots, 5$ ) can be classified as one of modified gravitational theories.

The full cosmological dynamics including the terms up to  $\mathcal{L}_5$  have been studied by two of the present authors in the flat Friedmann-Lemaitre-Robertson-Walker (FLRW) background [23, 24] (see also Refs. [25]-[45] for related works). While the field is nearly frozen during the early epoch through the cosmological Vainshtein mechanism, it begins to evolve at late times to lead to the acceleration of the Universe. The stable dS solution can be realized by a constant field velocity.

Refs. [23, 24] have shown that, for the covariant Galileon theory having dS attractors, cosmological solutions with different initial conditions converge to a common trajectory— a tracker solution. Moreover the background cosmological dynamics along the tracker can be known analytically in terms of the redshift  $z$ . The dark energy equation of state exhibits the peculiar phantom-like evolution:  $w_{\text{DE}} = -7/3$  (radiation era),  $w_{\text{DE}} = -2$  (matter era), and  $w_{\text{DE}} = -1$  (dS era). Note that this does not imply the appearance of ghosts. In fact the viable model parameter space has been found in Refs. [23, 24] from the conditions to avoid ghosts and Laplacian instabilities of scalar and tensor perturbations.

In this paper we place observational constraints on the covariant Galileon gravity using the observational data of SN Ia, the CMB shift parameters, and BAO. In particular we derive a convenient analytic formula for the tracker evolution by including the cosmic curvature  $K$  and test the viability of such a solution. In general the cosmological dynamics start from the regime away from the tracker, depending on the model parameters and initial conditions. We shall also study such general cases and search for the model parameter space consistent with observational constraints.

## II. GALILEON COSMOLOGY

The covariant Galileon gravity is described by the action [22]

$$S = \int d^4x \sqrt{-g} \left[ \frac{M_{\text{pl}}^2}{2} R + \frac{1}{2} \sum_{i=1}^5 c_i \mathcal{L}_i \right] + \int d^4x \mathcal{L}_M, \quad (1)$$

where  $g$  is a determinant of the metric tensor  $g_{\mu\nu}$ ,  $M_{\text{pl}}$  is the reduced Planck mass, and  $c_i$  are constants. The covariant Lagrangians  $\mathcal{L}_i$  ( $i = 1, \dots, 5$ ) that respect the Galilean symmetry in the limit of the Minkowski space-

time are given by

$$\begin{aligned} \mathcal{L}_1 &= M^3 \phi, & \mathcal{L}_2 &= (\nabla\phi)^2, & \mathcal{L}_3 &= (\square\phi)(\nabla\phi)^2/M^3, \\ \mathcal{L}_4 &= (\nabla\phi)^2 [2(\square\phi)^2 - 2\phi_{;\mu\nu}\phi^{;\mu\nu} - R(\nabla\phi)^2/2]/M^6, \\ \mathcal{L}_5 &= (\nabla\phi)^2 [(\square\phi)^3 - 3(\square\phi)\phi_{;\mu\nu}\phi^{;\mu\nu} \\ &\quad + 2\phi_{;\mu}{}^\nu\phi_{;\nu}{}^\rho\phi_{;\rho}{}^\mu - 6\phi_{;\mu}\phi^{;\mu\nu}\phi^{;\rho}G_{\nu\rho}]/M^9, \end{aligned} \quad (2)$$

where a semicolon represents a covariant derivative,  $M$  is a constant having a dimension of mass, and  $G_{\nu\rho}$  is the Einstein tensor. For the matter Lagrangian  $\mathcal{L}_M$  we take into account perfect fluids of radiation (energy density  $\rho_r$ , equation of state  $w_r = 1/3$ ) and non-relativistic matter (energy density  $\rho_m$ , equation of state  $w_m = 0$ ).

We consider the FLRW space-time with the line element

$$ds^2 = -dt^2 + a^2(t) \left[ \frac{dr^2}{1 - Kr^2} + r^2(d\theta^2 + \sin^2\theta d\phi^2) \right], \quad (3)$$

where  $a(t)$  is the scale factor with the cosmic time  $t$ . The closed, flat, and open geometries correspond to  $K > 0$ ,  $K = 0$ , and  $K < 0$ , respectively. Variation of the action (1) with respect to  $g_{\mu\nu}$  leads to the following equations of motion

$$3M_{\text{pl}}^2 H^2 = \rho_{\text{DE}} + \rho_m + \rho_r + \rho_K, \quad (4)$$

$$3M_{\text{pl}}^2 H^2 + 2M_{\text{pl}}^2 \dot{H} = -P_{\text{DE}} - \rho_r/3 + \rho_K/3, \quad (5)$$

$$\dot{\rho}_m + 3H\rho_m = 0, \quad (6)$$

$$\dot{\rho}_r + 4H\rho_r = 0, \quad (7)$$

where  $\rho_K \equiv -3KM_{\text{pl}}^2/a^2$ , a dot represents a derivative with respect to  $t$ ,  $H = \dot{a}/a$  is the Hubble parameter, and

$$\begin{aligned} \rho_{\text{DE}} &\equiv -c_1 M^3 \phi/2 - c_2 \dot{\phi}^2/2 + 3c_3 H \dot{\phi}^3/M^3 \\ &\quad - 45c_4 H^2 \dot{\phi}^4/(2M^6) + 21c_5 H^3 \dot{\phi}^5/M^9, \end{aligned} \quad (8)$$

$$\begin{aligned} P_{\text{DE}} &\equiv c_1 M^3 \phi/2 - c_2 \dot{\phi}^2/2 - c_3 \dot{\phi}^2 \ddot{\phi}/M^3 \\ &\quad + 3c_4 \dot{\phi}^3 [8H\ddot{\phi} + (3H^2 + 2\dot{H})\dot{\phi}]/(2M^6) \\ &\quad - 3c_5 H \dot{\phi}^4 [5H\ddot{\phi} + 2(H^2 + \dot{H})\dot{\phi}]/M^9. \end{aligned} \quad (9)$$

Note that Eqs. (4) and (5) are the generalization of those derived in Ref. [23] with an account of the cosmic curvature  $K$ . The closed-form equations for  $\ddot{\phi}$  and  $\dot{H}$  can be derived by taking a time-derivative of Eq. (4) and by combining it with Eq. (5). Since we are interested in the case where the late-time cosmic acceleration is realized by the field kinetic energy, we set  $c_1 = 0$  in the following discussion. In this case the only solution in the Minkowski background ( $H = 0$ ) corresponds to  $\dot{\phi} = 0$  for  $c_2 \neq 0$ .

The dS solution ( $H = H_{\text{dS}} = \text{constant}$ ) can be present for  $\dot{\phi} = \dot{\phi}_{\text{dS}} = \text{constant}$ . We normalize the mass  $M$  to be  $M^3 = M_{\text{pl}} H_{\text{dS}}^2$ , which gives  $M \approx 10^{-40} M_{\text{pl}}$  for  $H_{\text{dS}} \approx 10^{-60} M_{\text{pl}}$ . Defining  $x_{\text{dS}} \equiv \dot{\phi}_{\text{dS}}/(H_{\text{dS}} M_{\text{pl}})$ , Eqs. (4) and (5) give the following relations at the dS point:

$$c_2 x_{\text{dS}}^2 = 6 + 9\alpha - 12\beta, \quad (10)$$

$$c_3 x_{\text{dS}}^3 = 2 + 9\alpha - 9\beta, \quad (11)$$

where

$$\alpha \equiv c_4 x_{\text{dS}}^4, \quad \beta \equiv c_5 x_{\text{dS}}^5. \quad (12)$$

The use of  $\alpha$  and  $\beta$  is convenient because the coefficients of physical quantities and dynamical equations can be expressed by those variables. We note that the relations (10) and (11) are not subject to change under the rescaling  $x_{\text{dS}} \rightarrow \gamma x_{\text{dS}}$  and  $c_i \rightarrow c_i/\gamma^i$ , where  $\gamma$  is a real constant. Hence the rescaled choice of  $c_i$  can provide the same physics. If we use the parameters  $\alpha$  and  $\beta$ , such apparent different cases can be treated in a unified way. In Refs. [23, 24] the authors derived the viable parameter space on the  $(\alpha, \beta)$  plane in which the conditions for the avoidance of ghosts and Laplacian instabilities of scalar and tensor perturbations are satisfied for  $K = 0$ .

In order to study the cosmological dynamics, it is useful to define the following dimensionless variables:

$$r_1 \equiv \frac{\dot{\phi}_{\text{dS}} H_{\text{dS}}}{\dot{\phi} H}, \quad r_2 \equiv \frac{1}{r_1} \left( \frac{\dot{\phi}}{\dot{\phi}_{\text{dS}}} \right)^4. \quad (13)$$

At the dS solution one has  $r_1 = 1$  and  $r_2 = 1$ . We define the dark energy density parameter

$$\begin{aligned} \Omega_{\text{DE}} &\equiv \frac{\rho_{\text{DE}}}{3M_{\text{pl}}^2 H^2} \\ &= -(2 + 3\alpha - 4\beta)r_1^3 r_2/2 + (2 + 9\alpha - 9\beta)r_1^2 r_2 \\ &\quad - 15\alpha r_1 r_2/2 + 7\beta r_2, \end{aligned} \quad (14)$$

where we have used Eqs. (10) and (11). Then Eq. (4) can be written as

$$\Omega_{\text{DE}} + \Omega_m + \Omega_r + \Omega_K = 1, \quad (15)$$

where  $\Omega_m \equiv \rho_m/(3M_{\text{pl}}^2 H^2)$ ,  $\Omega_r \equiv \rho_r/(3M_{\text{pl}}^2 H^2)$ , and  $\Omega_K \equiv \rho_K/(3M_{\text{pl}}^2 H^2) = -K/(aH)^2$ .

From Eqs. (4)-(7) we obtain the following autonomous equations for the variables  $r_1$ ,  $r_2$ ,  $\Omega_r$ , and  $\Omega_K$ :

$$\begin{aligned} r_1' &= \frac{1}{\Delta} (r_1 - 1) r_1 [r_1 (r_1 (-3\alpha + 4\beta - 2) + 6\alpha - 5\beta) - 5\beta] \\ &\quad \times [2(\Omega_r - \Omega_K + 9) + 3r_2 (r_1^3 (-3\alpha + 4\beta - 2) + 2r_1^2 (9\alpha - 9\beta + 2) - 15r_1 \alpha + 14\beta)], \end{aligned} \quad (16)$$

$$\begin{aligned} r_2' &= -\frac{1}{\Delta} [r_2 (6r_1^2 (r_2 (45\alpha^2 - 4(9\alpha + 2)\beta + 36\beta^2) - (\Omega_r - \Omega_K - 7)(9\alpha - 9\beta + 2)) + r_1^3 (-2(\Omega_r - \Omega_K + 33) \\ &\quad \times (3\alpha - 4\beta + 2) - 3r_2 (-2(201\alpha + 89)\beta + 15\alpha(9\alpha + 2) + 356\beta^2)) - 3r_1 \alpha (-28\Omega_r + 28\Omega_K + 123r_2 \beta + 36) \\ &\quad + 10\beta (-11\Omega_r + 11\Omega_K + 21r_2 \beta - 3) + 3r_1^4 r_2 (9\alpha^2 - 30\alpha(4\beta + 1) + 2(2 - 9\beta)^2) + 3r_1^6 r_2 (3\alpha - 4\beta + 2)^2 \\ &\quad + 3r_1^5 r_2 (9\alpha - 9\beta + 2)(3\alpha - 4\beta + 2)], \end{aligned} \quad (17)$$

$$\Omega_r' = \Omega_r \left( -4 - 2\frac{H'}{H} \right), \quad (18)$$

$$\Omega_K' = \Omega_K \left( -2 - 2\frac{H'}{H} \right), \quad (19)$$

where a prime represents a derivative with respect to  $N = \ln a$ , and

$$\begin{aligned} \Delta &\equiv 2r_1^4 r_2 [72\alpha^2 + 30\alpha(1 - 5\beta) + (2 - 9\beta)^2] + 4r_1^2 [9r_2 (5\alpha^2 + 9\alpha\beta + (2 - 9\beta)\beta) + 2(9\alpha - 9\beta + 2)] \\ &\quad + 4r_1^3 [-3r_2 (-2(15\alpha + 1)\beta + 3\alpha(9\alpha + 2) + 4\beta^2) - 3\alpha + 4\beta - 2] - 24r_1 \alpha (16r_2 \beta + 3) + 10\beta (21r_2 \beta + 8). \end{aligned} \quad (20)$$

The Hubble parameter follows from the equation

$$\frac{H'}{H} = -\frac{5r_1'}{4r_1} - \frac{r_2'}{4r_2}. \quad (21)$$

The solutions to Eqs. (18) and (19) are given by  $\Omega_r(N) = \Omega_r^{(0)} e^{-4N} H_0^2/H^2(N)$  and  $\Omega_K(N) = \Omega_K^{(0)} e^{-2N} H_0^2/H^2(N)$  respectively, where the subscript “(0)” represents the values today ( $N = 0$  and  $a = 1$ ). Hence these variables are related with each other via

$$\Omega_K(N) = \Omega_K^{(0)} (\Omega_r(N)/\Omega_r^{(0)}) e^{2N}. \quad (22)$$

## A. Tracker solution

Equation (16) shows that there is an equilibrium point characterized by

$$r_1 = 1, \quad (23)$$

along which

$$\Omega_{\text{DE}} = r_2, \quad (24)$$

Originally the existence of the tracker solution (23) was found in Refs. [23, 24] for the flat Universe ( $K = 0$ ). The

above results show that the tracker is also present for  $K \neq 0$ .

The epoch at which the solutions reach the tracking regime  $r_1 \simeq 1$  depends on model parameters and initial conditions. The approach to this regime occurs later for smaller initial values of  $r_1$ . If  $r_1 \lesssim 2$  initially, numerical simulations show that the solutions approach the tracker with the late-time cosmic acceleration. Meanwhile, for the initial conditions with  $r_1 \gtrsim 2$ , the dominant contribution to  $\Omega_{\text{DE}}$  comes from the Lagrangian  $\mathcal{L}_2$ , so that the field energy density decreases rapidly as in the standard massless scalar field. In the latter case the solutions do not get out of the matter era that starts from the radiation-matter equality [23, 24].

From Eqs. (17)-(19) the variables  $r_2$ ,  $\Omega_r$ , and  $\Omega_K$  satisfy the following equations along the tracker:

$$r_2' = \frac{2r_2(3 - 3r_2 + \Omega_r - \Omega_K)}{1 + r_2}, \quad (25)$$

$$\Omega_r' = \frac{\Omega_r(\Omega_r - \Omega_K - 1 - 7r_2)}{1 + r_2}, \quad (26)$$

$$\Omega_K' = \frac{\Omega_K(\Omega_r - \Omega_K + 1 - 5r_2)}{1 + r_2}. \quad (27)$$

These equations do not have any dependence on  $\alpha$  and  $\beta$ . Combining Eqs. (25) and (26), we obtain

$$\frac{r_2'}{r_2} = 8 + \frac{2\Omega_r'}{\Omega_r}. \quad (28)$$

Integrating this equation, it follows that

$$r_2 = d_1 a^8 \Omega_r^2, \quad (29)$$

where  $d_1$  is a constant.

From Eqs. (26) and (27) we have

$$\frac{\Omega_K'}{\Omega_K} - \frac{\Omega_r'}{\Omega_r} = 2, \quad (30)$$

which is integrated to give

$$\frac{\Omega_K}{\Omega_r} = d_2 a^2, \quad \text{with} \quad d_2 = \frac{\Omega_K^{(0)}}{\Omega_r^{(0)}}. \quad (31)$$

Substituting Eqs. (29) and (31) into Eq. (26), we obtain the following integrated solution

$$\Omega_r = \frac{-1 + d_3 a - d_2 a^2 + \sqrt{4d_1 a^8 + (-1 + d_3 a - d_2 a^2)^2}}{2d_1 a^8}, \quad (32)$$

where  $d_3$  is another constant. Note that another solution of  $\Omega_r$  (i.e. minus sign in front of the square root) is not cosmologically viable, because of the divergence of  $\Omega_r$  as  $a \rightarrow 0$ . The density parameter (32) evolves as  $\Omega_r \simeq 1 + d_3 a$  in the early time ( $a \ll 1$ ). This demands the condition  $d_3 < 0$  provided that  $\Omega_{\text{DE}} > 0$ .

Using the density parameters  $\Omega_m^{(0)}$ ,  $\Omega_r^{(0)}$ , and  $\Omega_K^{(0)}$  today, the constants  $d_1$  and  $d_3$  can be expressed as

$$d_1 = \frac{1 - \Omega_m^{(0)} - \Omega_r^{(0)} - \Omega_K^{(0)}}{(\Omega_r^{(0)})^2}, \quad d_3 = -\frac{\Omega_m^{(0)}}{\Omega_r^{(0)}}, \quad (33)$$

where we have used Eqs. (15), (24), and (32). In the high-redshift regime ( $z \gg 1$ ) the density parameters behave as  $\Omega_{\text{DE}} \simeq d_1 / [(1+z)^6 (1+z-d_3)^2]$ ,  $\Omega_r \simeq (1+z)/(1+z-d_3)$ , and  $\Omega_K \simeq d_2 / [(1+z)(1+z-d_3)]$ .

Since  $\Omega_r \propto \rho_r / H^2 \propto 1/(a^4 H^2)$ , it follows that  $H^2 / H_0^2 = (\Omega_r^{(0)} / \Omega_r) (1/a^4)$ . Using Eqs. (32) and (33), the Hubble parameter can be expressed in terms of the function of the redshift  $z = 1/a - 1$ :

$$\left(\frac{H(z)}{H_0}\right)^2 = \frac{1}{2}\Omega_K^{(0)}(1+z)^2 + \frac{1}{2}\Omega_m^{(0)}(1+z)^3 + \frac{1}{2}\Omega_r^{(0)}(1+z)^4 + \sqrt{1 - \Omega_m^{(0)} - \Omega_r^{(0)} - \Omega_K^{(0)} + \frac{(1+z)^4}{4} \left[ \Omega_K^{(0)} + \Omega_m^{(0)}(1+z) + \Omega_r^{(0)}(1+z)^2 \right]^2}. \quad (34)$$

This analytic estimation is useful to constrain the tracker solution from a number of observations.

On the tracker the equation of state of dark energy  $w_{\text{DE}} \equiv P_{\text{DE}}/\rho_{\text{DE}}$  and the effective equation of state

$w_{\text{eff}} \equiv -1 - 2\dot{H}/(3H^2)$  are given by

$$w_{\text{DE}} = -\frac{\Omega_r - \Omega_K + 6}{3(r_2 + 1)}, \quad (35)$$

$$w_{\text{eff}} = \frac{\Omega_r - \Omega_K - 6r_2}{3(r_2 + 1)}. \quad (36)$$

During the cosmological sequence of radiation ( $\Omega_r \simeq 1$ ,  $|\Omega_K| \ll 1$ ,  $r_2 \ll 1$ ), matter ( $\Omega_r \ll 1$ ,  $|\Omega_K| \ll 1$ ,

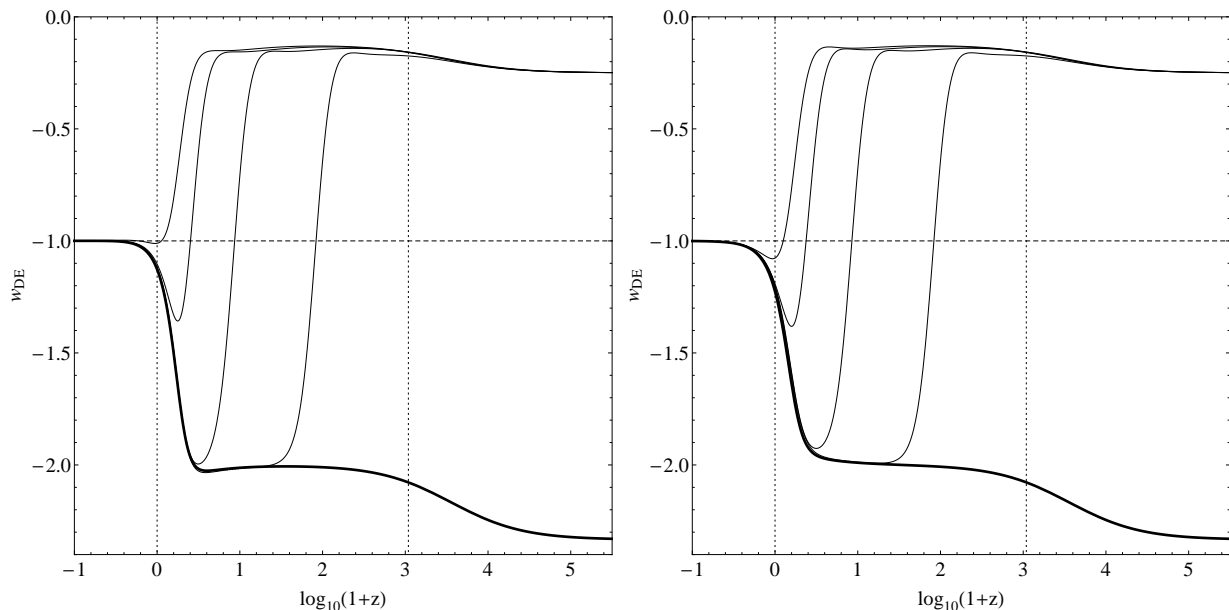


Figure 1: The evolution of the dark energy equation of state  $w_{\text{DE}}$  versus the redshift  $z$  for  $\Omega_K^{(0)} = -0.1$  (left) and  $\Omega_K^{(0)} = 0.1$  (right) with  $\alpha = 0.3$  and  $\beta = 0.14$ . We choose the initial conditions as those given in the caption of figure 3 of Ref. [24]. The tracker solution ( $r_1 = 1$ ) is shown as a bold line. For given  $\Omega_r(N)$ , the curvature density parameter  $\Omega_K(N)$  is determined according to Eq. (22). The two vertical lines denote the present time ( $z = 0$ ) and the epoch at decoupling  $z = z_*$ , while the horizontal line corresponds to the  $\Lambda$ CDM model ( $w_{\text{DE}} = -1$ ).

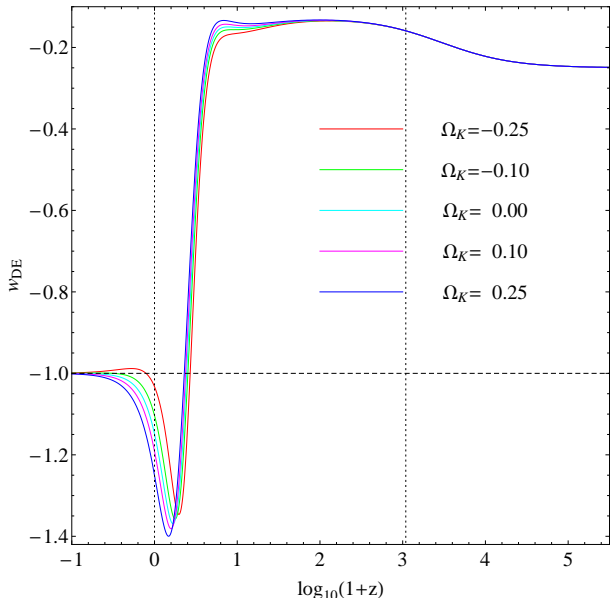


Figure 2: The evolution of  $w_{\text{DE}}$  for  $\alpha = 0.3$  and  $\beta = 0.14$  with various values of the cosmic curvature:  $\Omega_K^{(0)} = (-0.25, -0.1, 0, 0.1, 0.25)$ . The initial conditions are chosen to be  $r_1 = 1.5 \times 10^{-10}$ ,  $r_2 = 2.667 \times 10^{-12}$ ,  $\Omega_r = 0.999992$  at  $z = 3.63 \times 10^8$  [where  $N = -\ln(1+z)$ ]. The meaning of two vertical lines and the horizontal line is the same as in Fig. 1.

$r_2 \ll 1$ ), and dS ( $\Omega_r \ll 1$ ,  $|\Omega_K| \ll 1$ ,  $r_2 = 1$ ) eras, the dark energy equation of state shows peculiar evolution:  $w_{\text{DE}} = -7/3 \rightarrow -2 \rightarrow -1$ , whereas the effective

equation of state evolves as  $w_{\text{eff}} = 1/3 \rightarrow 0 \rightarrow -1$ . If the curvature density parameter  $\Omega_K$  is non-negligible today, this also gives some contribution to  $w_{\text{DE}}$  and  $w_{\text{eff}}$  during the evolution from the end of the matter era to the present epoch. In Fig. 1 the evolution of the tracker solution (shown as a bold line) for  $\Omega_K^{(0)} = -0.1$  does not look very much different from that for  $\Omega_K^{(0)} = 0.1$ . We caution, however, that inclusion of the cosmic curvature changes the diameter distance as well as the luminosity distance relative to the flat Universe.

The conditions for the avoidance of ghosts and instabilities have been derived in Refs. [23, 24] for  $\Omega_K = 0$ . Even in the presence of the cosmic curvature it is a good approximation to use the results in the flat case, because  $\Omega_K$  is much smaller than 1 in most of the expansion history of the Universe. Hence we shall use the allowed region in the  $(\alpha, \beta)$  plane shown in the figure 1 of Ref. [23].

## B. General solutions

There is another case in which the solutions start to evolve from the regime  $r_1 \ll 1$ . If  $r_1 \ll 1$  initially, the ghosts are absent for  $\beta > 0$  [23, 24]. Provided that  $r_1 \ll 1$  the propagation speeds of scalar and tensor perturbations are positive during radiation and matter eras, so that no instabilities are present.

In the regime  $r_1 \ll 1$ , the variables  $r_1$  and  $r_2$  satisfy

the following approximate equations

$$r_1' \simeq \frac{9 + \Omega_r - \Omega_K + 21\beta r_2}{8 + 21\beta r_2} r_1, \quad (37)$$

$$r_2' \simeq \frac{3 + 11\Omega_r - 11\Omega_K - 21\beta r_2}{8 + 21\beta r_2} r_2. \quad (38)$$

As long as  $\{\beta r_2, |\Omega_K|\} \ll 1$ , the evolution of  $r_1$  and  $r_2$  during the radiation (matter) era is given by  $r_1 \propto a^{5/4}$  and  $r_2 \propto a^{7/4}$  ( $r_1 \propto a^{9/8}$  and  $r_2 \propto a^{3/8}$ ). Hence the field velocity evolves as  $\dot{\phi} \propto t^{3/8}$  during the radiation era and  $\dot{\phi} \propto t^{1/4}$  during the matter era. Note that the evolution of  $\dot{\phi}$  is slower than that for the tracker (i.e.  $\dot{\phi} \propto t$ ).

In Ref. [24] it was shown that the tracker is stable in the direction of  $r_1$  by considering a homogeneous perturbation  $\delta r_1$ . This means that once the solutions reach the tracker the variable  $r_1$  does not repel away from 1. The epoch at which the solutions approach the tracker regime depends on the initial values of  $r_1$ .

The dark energy equation of state  $w_{\text{DE}}$  and the effective equation of state  $w_{\text{eff}}$  in the regime  $r_1 \ll 1$  are approximately given by

$$w_{\text{DE}} \simeq -\frac{1 + \Omega_r - \Omega_K}{8 + 21\beta r_2}, \quad (39)$$

$$w_{\text{eff}} \simeq \frac{8\Omega_r - 8\Omega_K - 21\beta r_2}{3(8 + 21\beta r_2)}. \quad (40)$$

Provided that  $\{\beta r_2, |\Omega_K|\} \ll 1$ , one has  $w_{\text{DE}} \simeq -1/4$ ,  $w_{\text{eff}} \simeq 1/3$  during the radiation era and  $w_{\text{DE}} \simeq -1/8$ ,  $w_{\text{eff}} \simeq 0$  during the matter era. The evolution of  $w_{\text{DE}}$  in the regime  $r_1 \ll 1$  is quite different from that for the tracker solution.

In Fig. 1 we plot the evolution of  $w_{\text{DE}}$  for a number of different initial conditions. Since  $r_1 \ll 1$  initially, the solutions start to evolve from the value  $w_{\text{DE}} \simeq -1/4$  in the radiation era. For larger initial values of  $r_1$  they approach the tracker earlier. This tracking behavior occurs irrespectively of the signs of  $\Omega_K^{(0)}$ . In Fig. 2 we find that the effect of the cosmic curvature slightly modifies the evolution of  $w_{\text{DE}}$  in the low-redshift regime.

### III. METHOD OF LIKELIHOOD ANALYSIS

In this section we show the method of our likelihood analysis to place observational constraints on the Galileon cosmology discussed above. The modified background cosmological evolution in this theory affects the diameter distance to the last scattering surface as well as the luminosity distance. The modification from the  $\Lambda$ CDM model can be tested by using the data of CMB, BAO and SN Ia.

#### A. CMB shift parameters

The positions of CMB acoustic peaks are affected by the expansion history of the Universe from the decoupling

epoch to today. In order to quantify the shift of acoustic peaks we use the data points  $(l_a, \mathcal{R}, z_*)$  of Ref. [5] (WMAP7), where  $l_a$  and  $\mathcal{R}$  are two CMB shift parameters [46–49] and  $z_*$  is the redshift at decoupling. For the FLRW metric (3) we have [50]

$$\mathcal{R} = \sqrt{\frac{\Omega_m^{(0)}}{\Omega_K^{(0)}}} \sinh \left( \sqrt{\Omega_K^{(0)}} \int_0^{z_*} \frac{dz}{H(z)/H_0} \right). \quad (41)$$

Numerically it is convenient to integrate the following equation from the redshift  $z = 0$  to  $z = z_*$ :

$$\frac{d\mathcal{R}}{dz} = \frac{1}{H(z)/H_0} \sqrt{\Omega_m^{(0)} + \mathcal{R}^2 \Omega_K^{(0)}}. \quad (42)$$

The multipole  $l_a$  is defined by  $l_a = \pi d_a^{(c)}(z_*)/r_s(z_*)$ , where  $d_a^{(c)}(z_*) = \mathcal{R}/(H_0 \sqrt{\Omega_m^{(0)}})$  is the comoving angular diameter distance and  $r_s(z_*) = \int_{z_*}^{\infty} dz / [\sqrt{3(1 + R_s(z))} H(z)]$  is the sound horizon at the decoupling. Note that  $R_s(z) = 3\Omega_b^{(0)}/[4\Omega_\gamma^{(0)}(1 + z)]$ , where  $\Omega_b^{(0)}$  and  $\Omega_\gamma^{(0)}$  are the today's density parameters of baryons and photons respectively. We neglect the contribution of dark energy and the cosmic curvature for  $z > z_*$  to estimate  $r_s(z_*)$ . The dark energy density parameter can be in fact neglected even for non-tracker solutions with  $r_1 \ll 1$ , because  $\Omega_{\text{DE}} \simeq 7\beta r_2$  decreases toward the past ( $r_2 \propto a^{3/8}$  during the matter era and  $r_2 \propto a^{7/4}$  during the radiation era). It then follows that (see e.g., [51])

$$l_a = \left[ \ln \left( \frac{\sqrt{R_s(z_*) + R_s(z_{\text{eq}})} + \sqrt{1 + R_s(z_*)}}{1 + \sqrt{R_s(z_{\text{eq}})}} \right) \right]^{-1} \times \frac{3\pi}{4} \sqrt{\frac{\Omega_b^{(0)}}{\Omega_\gamma^{(0)}}} \mathcal{R}. \quad (43)$$

For the redshift  $z_*$  there is a fitting formula by Hu and Sugiyama [52]:

$$z_* = 1048 (1 + 0.00124\omega_b^{-0.738}) (1 + g_1\omega_m^{g_2}), \quad (44)$$

where  $g_1 = 0.0783\omega_b^{-0.238}/(1 + 39.5\omega_b^{0.763})$ ,  $g_2 = 0.560/(1 + 21.1\omega_b^{1.81})$ ,  $\omega_b \equiv \Omega_b^{(0)}h^2$ , and  $\omega_m \equiv \Omega_m^{(0)}h^2$  ( $h$  correspond to the uncertainty of the Hubble parameter  $H_0$  today, i.e.  $H_0 = 100 h \text{ km sec}^{-1} \text{ Mpc}^{-1}$ ). The redshift at the radiation-matter equality is given by  $z_{\text{eq}} = \Omega_m^{(0)}/\Omega_r^{(0)} - 1$ .

For a flat prior, the 7-year WMAP data (WMAP7) measured best-fit values are [5]

$$\bar{\mathbf{V}}_{\text{CMB}} = \begin{pmatrix} \bar{l}_a \\ \bar{\mathcal{R}} \\ z_* \end{pmatrix} = \begin{pmatrix} 302.09 \pm 0.76 \\ 1.725 \pm 0.018 \\ 1091.3 \pm 0.91 \end{pmatrix}. \quad (45)$$

The corresponding inverse covariance matrix is [5]

$$\mathbf{C}_{\text{CMB}}^{-1} = \begin{pmatrix} 2.305 & 29.698 & -1.333 \\ 29.698 & 6825.270 & -113.180 \\ -1.333 & -113.180 & 3.414 \end{pmatrix}. \quad (46)$$

We thus define

$$\mathbf{X}_{\text{CMB}} = \begin{pmatrix} l_a - 302.09 \\ \mathcal{R} - 1.725 \\ z_* - 1091.3 \end{pmatrix}, \quad (47)$$

and construct the contribution of CMB to  $\chi^2$  as

$$\chi_{\text{CMB}}^2 = \mathbf{X}_{\text{CMB}}^T \mathbf{C}_{\text{CMB}}^{-1} \mathbf{X}_{\text{CMB}}. \quad (48)$$

Notice that  $\chi_{\text{CMB}}^2$  depends on the parameters  $(\Omega_m^{(0)}, \Omega_b^{(0)}, h)$ . In the analysis of the Galileon model we use the priors  $h = 0.71$  and  $\Omega_b^{(0)} = 0.02258 h^{-2}$  [5]. As we shall see later on, varying  $h$  does not affect the final results of our study. The density parameter of radiation today is

$$\Omega_r^{(0)} = \Omega_\gamma^{(0)}(1 + 0.2271 N_{\text{eff}}), \quad (49)$$

where  $\Omega_\gamma^{(0)}$  is the photon density parameter and  $N_{\text{eff}}$  is the relativistic degrees of freedom. We adopt the standard values  $\Omega_\gamma^{(0)} = 2.469 \times 10^{-5} h^{-2}$  and  $N_{\text{eff}} = 3.04$  [5].

In Ref. [46] Wang and Mukherjee placed observational constraints on  $\mathcal{R}$  and  $l_a$  for several different dark energy models: the  $\Lambda$ CDM model, constant  $w_{\text{DE}}$  models, and the models described by the parametrization  $w_{\text{DE}} = w_0 + w_a(1 - a)$ . They showed that the resulting bounds on  $\mathcal{R}$  and  $l_a$  are independent of the dark energy models. While our Galileon model does not belong to the models described above, the method using the two distance measures  $\mathcal{R}$  and  $l_a$  is expected to be trustable as well. In fact the Galileon model is consistent with a number of assumptions [53] that validate the analysis using the two WMAP distance priors.

## B. BAO

For the BAO we apply the maximum likelihood method [48] using the data points of Ref. [4] (SDSS7):

$$\bar{\mathbf{V}}_{\text{BAO}} = \begin{pmatrix} \frac{r_s(z_d)}{D_V(0.2)} = 0.1905 \pm 0.0061 \\ \frac{r_s(z_d)}{D_V(0.35)} = 0.1097 \pm 0.0036 \end{pmatrix}, \quad (50)$$

where  $r_s(z_d)$  is the sound horizon at the baryon drag epoch  $z_d$ . For  $z_d$  we use the fitting formula by Eisenstein and Hu [54]:

$$z_d = \frac{1291 \omega_m^{0.251}}{1 + 0.659 \omega_m^{0.828}} \left(1 + b_1 \omega_b^{b_2}\right), \quad (51)$$

where  $b_1 = 0.313 \omega_m^{-0.419} (1 + 0.607 \omega_m^{0.674})$  and  $b_2 = 0.238 \omega_m^{0.223}$ . The dilation scale  $D_V$  at the redshift  $z$  is

$$D_V(z) = \left[ (1+z)^2 d_A^2(z) \frac{z}{H(z)} \right]^{1/3}, \quad (52)$$

where  $d_A(z)$  is the diameter distance defined by

$$d_A(z) = \frac{1}{1+z} \frac{1}{H_0 \sqrt{\Omega_K^{(0)}}} \sinh \left( \sqrt{\Omega_K^{(0)}} \int_0^z \frac{d\tilde{z}}{H(\tilde{z})/H_0} \right). \quad (53)$$

This encodes the visual distortion of a spherical object due to the non-euclidianity of the FLRW space-time, which is equivalent to the geometric mean of the distortion along the line of sight and two orthogonal directions.

We thus construct

$$\mathbf{X}_{\text{BAO}} = \begin{pmatrix} \frac{r_s(z_d)}{D_V(0.2)} - 0.1905 \\ \frac{r_s(z_d)}{D_V(0.35)} - 0.1097 \end{pmatrix}, \quad (54)$$

and using the inverse covariance matrix [4]

$$\mathbf{C}_{\text{BAO}}^{-1} = \begin{pmatrix} 30124 & -17227 \\ -17227 & 86977 \end{pmatrix}. \quad (55)$$

The contribution of BAO to  $\chi^2$  is

$$\chi_{\text{BAO}}^2 = \mathbf{X}_{\text{BAO}}^T \mathbf{C}_{\text{BAO}}^{-1} \mathbf{X}_{\text{BAO}}. \quad (56)$$

## C. SN Ia

The analysis of SN Ia standard candles is based on the method described in Ref. [48]. We will mainly use the Constitution SN Ia dataset of Hicken *et al.* [55], which constitutes in total of 397 SN Ia. We will also use the recently released update to the Union set, i.e. the Union2 dataset [56].

The SN Ia observations use light curve fitters to provide the apparent magnitude  $m(z)$  of the supernovae at peak brightness. This is related with the luminosity distance  $d_L(z)$  through  $m(z) = M + 5 \log_{10}(d_L/10 \text{ pc})$ , where  $M$  is the absolute magnitude. Note that the luminosity distance is given by

$$d_L(z) = (1+z)^2 d_A(z), \quad (57)$$

where  $d_A(z)$  is the angular diameter distance defined in Eq. (53). Defining the dimensionless luminosity distance as  $\bar{d}_L(z) \equiv d_L(z)/H_0^{-1}$ , the theoretical value of the apparent magnitude is

$$m_{\text{th}}(z) = \bar{M}(M, H_0) + 5 \log_{10}(\bar{d}_L(z)), \quad (58)$$

where  $\bar{M} = M - 5 \log_{10} h + 42.38$  [48].

The theoretical model parameters are determined by minimizing the quantity

$$\chi_{\text{SN Ia}}^2(\Omega_m^{(0)}, p_j) = \sum_{i=1}^N \frac{[\mu_{\text{obs}}(z_i) - \mu_{\text{th}}(z_i)]^2}{\sigma_{\mu i}^2}, \quad (59)$$

where  $N$  is the number of the SN Ia dataset,  $p_j$  is the set of parameters to be fitted, and  $\sigma_{\mu i}^2$  are the errors due to flux uncertainties, intrinsic dispersion of SN Ia absolute

magnitude and peculiar velocity dispersion. These errors are assumed to be Gaussian and uncorrelated. The theoretical distance modulus is defined as

$$\mu_{\text{th}}(z_i) \equiv m_{\text{th}}(z_i) - M = 5 \log_{10}(\bar{d}_L(z)) + \mu_0, \quad (60)$$

where  $\mu_0 = 42.38 - 5 \log_{10} h$ . The steps we have followed for the usual minimization of (59) in terms of its parameters are described in detail in Refs. [57–59].

#### D. Two information criteria

In order to see whether the Galileon model is favored over the  $\Lambda$ CDM model, we will also use the two information criteria known as AIC (Akaike Information Criterion) and BIC (Bayesian Information Criterion), see Ref. [60] and references there in. The AIC is defined as

$$\text{AIC} = -2 \ln \mathcal{L}_{\text{max}} + 2k, \quad (61)$$

where the likelihood is defined as  $\mathcal{L} \propto e^{-\chi^2/2}$ , the term  $-2 \ln \mathcal{L}_{\text{max}}$  corresponds to the minimum  $\chi^2$ , and  $k$  is the number of parameters of the model. The BIC is defined similarly as

$$\text{BIC} = -2 \ln \mathcal{L}_{\text{max}} + k \ln N, \quad (62)$$

where  $N$  is the number of data points in the set under consideration.

According to these criteria a model with the smaller AIC/BIC is considered to be the best and specifically, for the BIC a difference of 2 is considered as positive evidence, while 6 or more as strong evidence in favor of the model with the smaller value. Similarly, for the AIC a difference in the range between 0 and 2 means that the two models have about the same support from the data as the best one, for a difference in the range between 2 and 4 this support is considerably less for the model with the larger AIC, while for a difference  $> 10$  the model with the larger AIC is practically irrelevant [60, 61].

### IV. OBSERVATIONAL CONSTRAINTS

In this section we present the observational constraints on the Galileon cosmology. We first consider the tracker solution and later we study general solutions discussed in Sec. II B. In the latter case we shall explore the whole parameter space in terms of  $(\alpha, \beta)$  constrained by the conditions for the avoidance of ghosts and instabilities (figure 1 in Ref. [23]).

#### A. The tracker

As we showed in Eq. (34), the Hubble parameter for the tracker is known as a function of the redshift  $z$ . Since the value of  $\Omega_r^{(0)}$  is fixed from the CMB [see Eq. (49)], the

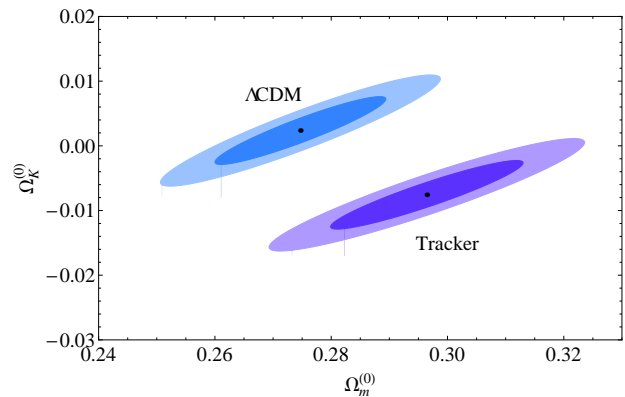


Figure 3: The 68.3% ( $1\sigma$ )–95.4% ( $2\sigma$ )  $\chi^2$  confidence contours in the  $(\Omega_m^{(0)}, \Omega_K^{(0)})$  plane for (i) the tracker model and (ii) the  $\Lambda$ CDM model. Both contours correspond to the combination of all three datasets, i.e. Constitution SN Ia+BAO+CMB. The best fit parameters are found in Table I. The difference in  $\chi^2$  between the two models is  $\delta\chi^2 \sim 22$ , which corresponds to  $\sim 4.3\sigma$ . Hence the tracker model is severely disfavored with respect to the  $\Lambda$ CDM model.

tracker has only two free parameters  $\Omega_m^{(0)}$  and  $\Omega_K^{(0)}$ . In what follows the priors  $h = 0.71$  and  $\Omega_b^{(0)} = 0.02258 h^{-2}$  [5] are used in order to simplify the analysis. We have checked that having  $h$  as a free parameter for the likelihood analysis of the CMB and BAO does not change the results much, as the best fits are always within 1%.

We should also mention that we have not solved the full perturbation equations for the Galileon field in order to calculate the effect on the CMB. However, the modified growth of perturbations only affects the large-scale CMB spectrum (the multipoles  $l \lesssim 10$ ) through the Integrated-Sachs-Wolfe (ISW) effect. Usually this does not provide tighter constraints than the CMB distance measures explained in Sec. III A. Hence we expect that the results are not subject to change much.

In Table I we show a comparison of the tracker given in Eq. (34) to the  $\Lambda$ CDM model for various data combinations. If we only use either of the SN Ia data (Constitution or Union2), the  $\chi^2$  for the tracker is similar to that in the  $\Lambda$ CDM for both the flat and non-flat cases. Hence the two models are practically indistinguishable from each other. The tracker solution is also consistent with the individual observational constraint from either CMB or BAO. The combined data analysis of CMB+BAO shows that, as long as we take into account the cosmic curvature, the  $\chi^2$  for the tracker is even smaller than that in the  $\Lambda$ CDM.

In Fig. 3 we plot the  $\chi^2 (= \chi_{\text{SN}}^2 + \chi_{\text{CMB}}^2 + \chi_{\text{BAO}}^2)$  confidence contours in the  $(\Omega_m^{(0)}, \Omega_K^{(0)})$  plane at the 68.3% ( $1\sigma$ ) – 95.4% ( $2\sigma$ ) levels. Both contours correspond to the combination of all three datasets: Constitution SN Ia+BAO+CMB. As we see in Table I, the difference in  $\chi^2$  between the two models is  $\delta\chi^2 \sim 22$ . This corresponds to  $\sim 4.3\sigma$ , and the tracker solution is



Table I: Comparison of the tracker solution characterized by (34) to the  $\Lambda$ CDM model for various data combinations. If we use the SN Ia data alone, the model is practically indistinguishable from the  $\Lambda$ CDM. However, if we add the CMB+BAO data, the tracker solution is disfavored relative to the  $\Lambda$ CDM. In all cases the error estimation is only statistical. In the cases where  $\Omega_K^{(0)} = 0$  it means that we assume the flat Universe in the data analysis.

Model (datasets)	$\chi_{\min}^2$	$\Omega_K^{(0)}$	$\Omega_m^{(0)}$
$\Lambda$ CDM (CMB)	0.22	0	$0.268 \pm 0.003$
Tracker (CMB)	16.50	0	$0.316 \pm 0.004$
$\Lambda$ CDM (CMB)	0.21	$0.000 \pm 0.004$	$0.27 \pm 0.01$
Tracker (CMB)	0.21	$-0.016 \pm 0.003$	$0.27 \pm 0.01$
$\Lambda$ CDM (BAO)	1.58	0	$0.306^{+0.047}_{-0.041}$
Tracker (BAO)	0.47	0	$0.263^{+0.039}_{-0.034}$
$\Lambda$ CDM (BAO)	0.00	$-0.37 \pm 0.23$	$0.22 \pm 0.06$
Tracker (BAO)	0.00	$-0.33 \pm 0.61$	$0.22 \pm 0.07$
$\Lambda$ CDM (CMB+BAO)	2.65	0	$0.268 \pm 0.004$
Tracker (CMB+BAO)	18.71	0	$0.316 \pm 0.004$
$\Lambda$ CDM (CMB+BAO)	2.56	$0.001 \pm 0.004$	$0.27 \pm 0.01$
Tracker (CMB+BAO)	0.67	$-0.016 \pm 0.26$	$0.27 \pm 0.12$
$\Lambda$ CDM (Constitution)	465.512	0	$0.289 \pm 0.022$
Tracker (Constitution)	465.508	0	$0.392 \pm 0.024$
$\Lambda$ CDM (Constitution)	465.353	$-0.09 \pm 0.23$	$0.325 \pm 0.092$
Tracker (Constitution)	465.423	$0.076 \pm 0.258$	$0.358 \pm 0.118$
$\Lambda$ CDM (Union2)	541.011	0	$0.269 \pm 0.020$
Tracker (Union2)	541.088	0	$0.369 \pm 0.022$
$\Lambda$ CDM (Union2)	540.879	$-0.07 \pm 0.19$	$0.296 \pm 0.076$
Tracker (Union2)	540.853	$0.106 \pm 0.217$	$0.324 \pm 0.097$
$\Lambda$ CDM (Constitution+BAO)	467.214	0	$0.269 \pm 0.020$
Tracker (Constitution+BAO)	472.729	0	$0.367 \pm 0.022$
$\Lambda$ CDM (Constitution+BAO)	466.721	$-0.052 \pm 0.074$	$0.306 \pm 0.028$
Tracker (Constitution+BAO)	467.066	$0.172 \pm 0.067$	$0.311 \pm 0.029$
$\Lambda$ CDM (Union2+BAO)	543.210	0	$0.277 \pm 0.018$
Tracker (Union2+BAO)	546.499	0	$0.349 \pm 0.020$
$\Lambda$ CDM (Union2+BAO)	542.013	$-0.077 \pm 0.071$	$0.296 \pm 0.027$
Tracker (Union2+BAO)	542.182	$0.148 \pm 0.066$	$0.303 \pm 0.028$
$\Lambda$ CDM (Constitution+BAO+CMB)	469.024	0	$0.269 \pm 0.004$
Tracker (Constitution+BAO+CMB)	494.397	0	$0.318 \pm 0.004$
$\Lambda$ CDM (Constitution+BAO+CMB)	468.543	$0.002 \pm 0.003$	$0.275 \pm 0.010$
Tracker (Constitution+BAO+CMB)	490.225	$-0.008 \pm 0.003$	$0.296 \pm 0.011$
$\Lambda$ CDM (Union2+BAO+CMB)	543.660	0	$0.268 \pm 0.003$
Tracker (Union2+BAO+CMB)	565.576	0	$0.318 \pm 0.004$
$\Lambda$ CDM (Union2+BAO+CMB)	543.582	$0.001 \pm 0.003$	$0.270 \pm 0.010$
Tracker (Union2+BAO+CMB)	560.183	$-0.008 \pm 0.003$	$0.294 \pm 0.011$

severely disfavored with respect to the  $\Lambda$ CDM. A similar conclusion is reached from the combined data analysis of Union2+BAO+CMB, which gives the difference of  $\delta\chi^2 \sim 16$  relative to the  $\Lambda$ CDM model.

The reason why the tracker is disfavored can be explained by inspecting Table I carefully. For the flat Universe the CMB data are practically incompatible with the tracker because of the peculiar evolution of  $w_{\text{DE}}$ . The main effect on the modification of the angular diameter distance to the last scattering surface comes from the contribution in the low-redshift regime ( $z \lesssim$  a few). In the non-flat background the CMB data are consistent with the tracker with the best fit values  $\Omega_m^{(0)} \sim 0.27$  and  $\Omega_K^{(0)} \sim -0.016$ . This value of  $\Omega_m^{(0)}$  is quite smaller than the SN Ia best fit ( $\Omega_m^{(0)} \gtrsim 0.32$ ), with either the Constitution or the Union2 datasets.

Regarding the SN Ia observations, the maximum redshift for the Constitution dataset is  $z_{\text{max}} = 1.551$  and  $z_{\text{max}} = 1.4$  for the Union2 dataset, while the average redshifts are  $z_{\text{mean}} = 0.4$  and  $z_{\text{mean}} = 0.35$  respectively. At  $z = 0.4$  and  $z = 1.4$  the dark energy equations of state are given by  $w_{\text{DE}} \sim -1.4$  and  $w_{\text{DE}} \sim -1.9$ , respectively. Since these values are away from  $w_{\text{DE}} = -1$ , the tracker can be compatible with the SN Ia data at the expense of choosing the values of  $\Omega_m^{(0)}$  larger than 0.3.

For the BAO datasets the best-fit value of  $\Omega_m^{(0)}$  in the non-flat Universe is even smaller ( $\Omega_m^{(0)} \sim 0.22$ ) than that constrained by the CMB shift parameters. Thus, as each dataset favors the value of  $\Omega_m^{(0)}$  in a different range, the combined analysis with all datasets does not favor the tracker solution.

## B. General solutions

Next, we proceed to observational constraints on the general solutions to Eqs. (16)-(19). Unlike the tracker solution, this case depends on the parameters  $\alpha$  and  $\beta$  as well as the initial conditions of  $r_1$ ,  $r_2$ , and  $\Omega_r$ . Note that the initial condition of  $\Omega_K$  is fixed by using Eq. (22). From Eq. (21) the Hubble parameter  $H(N)$  is integrated to give

$$\frac{H(N)}{H_0} = \left( \frac{r_1(0)}{r_1(N)} \right)^{5/4} \left( \frac{r_2(0)}{r_2(N)} \right)^{1/4}, \quad (63)$$

which can be used to compare the model with the data.

We place observational bound on  $(\alpha, \beta)$  constrained by the conditions for the avoidance of ghosts and instabilities. We also restrict  $\beta > 0$  to avoid the appearance of ghosts at the early cosmological epoch [23, 24]. Since the tracker is disfavored by the data, the cosmological evolution in which the solutions approach the tracker at late times (i.e. smaller initial values of  $r_1$ ) is in general favored. For given  $\alpha$  and  $\beta$ , we search for the viable initial conditions of  $r_1$ ,  $r_2$ , and  $\Omega_r$  that can be consistent with the data. We then carry out the likelihood analysis by varying  $\alpha$  and  $\beta$  to find the viable parameter space.

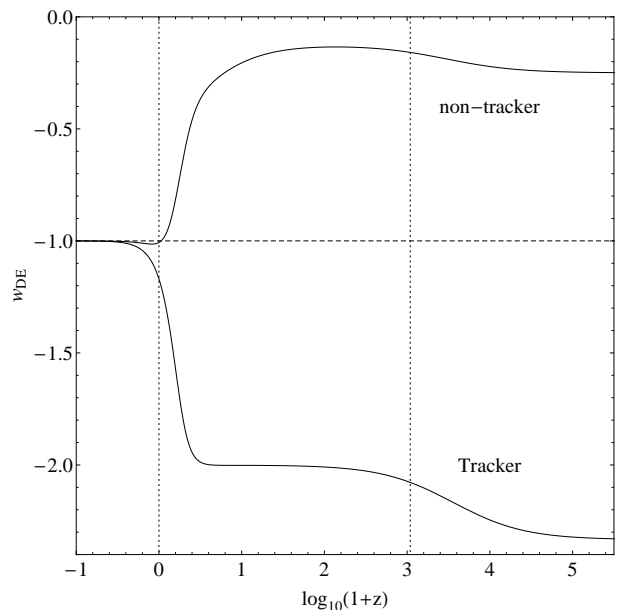


Figure 4: The evolution of the dark energy equation of state  $w_{\text{DE}}$  for the tracker solution (34) and the non-tracker case of Table II [denoted by an (\*), i.e.  $\alpha = 1.862$  and  $\beta = 0.607$  with the initial conditions given in the text]. The meaning of two vertical lines and the horizontal line is the same as in Fig. 1.

In Table II we show the best fit and the best fit parameters along their  $1\sigma$  errors and the AIC/BIC for several fixed values of  $\Omega_K^{(0)}$  ( $= 0, -0.01, 0.01$ ). According to the AIC statistics, the  $\Lambda$ CDM and the non-tracker solution with the positive curvature parameter  $\Omega_K^{(0)} = 0.01$  (with the best-fit values  $\alpha = 1.862$  and  $\beta = 0.607$ ) have more or less the same support. For this set of best-fit parameters we can always find a set of initial conditions for  $r_1$  and  $r_2$  that lead to the late-time tracker allowed by observations. For example, for the parameters  $\alpha = 1.862$  and  $\beta = 0.607$ , the initial conditions giving rise to the late-time tracker allowed by observations are  $r_1 = 1.50 \times 10^{-10} \pm 3.88 \times 10^{-12}$ ,  $r_2 = 2.67 \times 10^{-12} \pm 2.17 \times 10^{-13}$  (95 % CL), for  $\Omega_r = 0.999992$  at the redshift  $z = 3.63 \times 10^8$ . These conditions can be translated into the initial condition for  $\phi$  by using Eq. (13). In the case of  $\alpha = 1.862$  and  $\beta = 0.607$  it follows that  $4.38 \times 10^{-6} < \dot{\phi}/\dot{\phi}_{\text{dS}} < 4.57 \times 10^{-6}$  at  $z = 3.63 \times 10^8$ , thus requiring a certain amount of fine tuning.

For  $\Omega_K^{(0)} = -0.01$  the data support the  $\Lambda$ CDM model more, as the fit is particularly bad. On the other hand, according to the BIC statistics, there seems to be strong evidence in favor of the flat  $\Lambda$ CDM over all non-tracker cases as  $\Delta\text{BIC} \gtrsim 6$ .

In Fig. 4 we illustrate the evolution of  $w_{\text{DE}}$  for the solution denoted by an asterisk in Table II, together with the tracker solution. The former corresponds to the model parameters  $\alpha = 1.862$  and  $\beta = 0.607$  with the initial conditions  $r_1 = 1.5 \times 10^{-10}$ ,  $r_2 = 2.667 \times 10^{-12}$ , and

Table II: Comparison of general solutions of Eqs. (16)-(19) to the  $\Lambda$ CDM model for various data combinations and values of the curvature parameter  $\Omega_K^{(0)}$ . For the model that is denoted by an asterisk (\*), we show the evolution of  $w_{\text{DE}}$  in Fig. 4 (labeled as “non-tracker”).

Model/Data	$\chi^2_{\text{min}}$	Best fit parameters	AIC	$\Delta\text{AIC}$	AIC	$\Delta\text{BIC}$
(Constitution+BAO+CMB)						
$\Lambda\text{CDM}$ ( $\Omega_K^{(0)} = 0$ )	469.024	$\Omega_m^{(0)} = 0.269 \pm 0.004$	471.024	0	475.020	0
$\Lambda\text{CDM}$ ( $\Omega_K^{(0)} \neq 0$ )	468.543	$\Omega_K^{(0)} = 0.002 \pm 0.003$ $\Omega_m^{(0)} = 0.267 \pm 0.004$	472.543	1.519	480.536	5.515
$(\alpha, \beta)$ , ( $\Omega_K^{(0)} = 0$ )	470.912	$\alpha = 1.411 \pm 0.056$ $\beta = 0.422 \pm 0.022$	474.912	3.888	482.905	7.884
$(\alpha, \beta)$ , ( $\Omega_K^{(0)} = -0.01$ )	537.543	$\alpha = 0.956 \pm 0.079$ $\beta = 0.477 \pm 0.027$	541.543	70.519	549.536	74.515
(*) $(\alpha, \beta)$ , ( $\Omega_K^{(0)} = 0.01$ )	468.545	$\alpha = 1.862 \pm 0.058$ $\beta = 0.607 \pm 0.024$	472.545	1.521	480.538	5.517
$(\alpha, \beta, \Omega_m^{(0)}, \Omega_K^{(0)})$	468.311	$\alpha = 1.401 \pm 0.159$ $\beta = 0.425 \pm 0.064$ $\Omega_m^{(0)} = 0.287 \pm 0.014$ $\Omega_K^{(0)} = -0.003 \pm 0.005$	476.311	5.287	492.297	17.276
(Union2+BAO+CMB)						
$\Lambda\text{CDM}$ ( $\Omega_K^{(0)} = 0$ )	543.660	$\Omega_m^{(0)} = 0.268 \pm 0.003$	545.660	0	549.992	0
$\Lambda\text{CDM}$ ( $\Omega_K^{(0)} \neq 0$ )	543.582	$\Omega_K^{(0)} = 0.001 \pm 0.003$ $\Omega_m^{(0)} = 0.270 \pm 0.010$	547.582	1.922	556.245	6.254
$(\alpha, \beta)$ , ( $\Omega_K^{(0)} = 0$ )	543.895	$\alpha = 1.404 \pm 0.057$ $\beta = 0.419 \pm 0.023$	547.895	2.235	556.558	6.567
$(\alpha, \beta)$ , ( $\Omega_K^{(0)} = -0.01$ )	610.919	$\alpha = 0.956 \pm 0.089$ $\beta = 0.477 \pm 0.027$	614.919	69.259	623.582	73.591
$(\alpha, \beta)$ , ( $\Omega_K^{(0)} = 0.01$ )	543.646	$\alpha = 1.855 \pm 0.058$ $\beta = 0.603 \pm 0.024$	547.646	1.986	556.309	6.318
$(\alpha, \beta, \Omega_m^{(0)}, \Omega_K^{(0)})$	542.290	$\alpha = 1.401 \pm 0.779$ $\beta = 0.423 \pm 0.313$ $\Omega_m^{(0)} = 0.282 \pm 0.016$ $\Omega_K^{(0)} = -0.002 \pm 0.019$	550.290	4.630	567.616	17.625

$\Omega_r = 0.999992$  at  $z = 3.63 \times 10^8$ . In this case the solution does not reach the tracker by today and hence it does not exhibit strong phantom behavior. We find that the early tracking behavior is in fact disfavored by the combined data analysis.

The results in Table II for fixed  $\Omega_K^{(0)}$  imply that the generic solutions fare quite well for the open Universe (i.e. positive  $\Omega_K^{(0)}$ ), whereas they are not in good agreement with the data for the closed Universe with  $\Omega_K^{(0)} \lesssim -0.01$ . However, if we perform a general fit where all 4 parameters ( $\alpha, \beta, \Omega_m^{(0)}, \Omega_K^{(0)}$ ) are allowed to vary, then a slightly negative value of  $\Omega_K^{(0)}$  is favored, e.g.,  $\Omega_K^{(0)} = -0.003 \pm 0.005$  for the Constitution set. The reason why the general solutions are not particularly favored in the AIC and BIC tests lies in the fact that the number of parameters is larger than those in the flat  $\Lambda\text{CDM}$ . Therefore, we conclude that the general solutions exhibit rich phenomenology that can in general be in good agreement

with the combined observational constraints, while parts of the parameter space being in mild tension with the observations.

## V. CONCLUSIONS

In this paper we have placed observational constraints on the covariant Galileon cosmology by using the most recent data of SN Ia (Constitution and Union2 sets), CMB (WMAP7), and BAO (SDSS7). In this theory there is an interesting tracker solution that finally approaches a de Sitter solution responsible for dark energy. By including the cosmic curvature  $\Omega_K^{(0)}$ , we derived the analytic formula (34) about the evolution of the Hubble parameter for the tracker. This formula is convenient because we only need to vary the two density parameters  $\Omega_m^{(0)}$  and  $\Omega_K^{(0)}$  for the likelihood analysis as in the  $\Lambda\text{CDM}$  model

(with the radiation density parameter  $\Omega_r^{(0)}$  fixed by the CMB).

If we use either of the SN Ia data (Constitution or Union2) alone, the  $\chi^2$  for the tracker is similar to that in the  $\Lambda$ CDM model. We also found that, as long as the cosmic curvature is taken into account, the tracker solution is compatible with the individual observational bound constrained from either CMB or BAO. However, the combined data analysis of Constitution+BAO+CMB shows that the difference of  $\chi^2$  between the tracker and the  $\Lambda$ CDM is  $\delta\chi^2 \sim 22$  (or  $\sim 4.3\sigma$ ). Hence the tracker is severely disfavored with respect to the  $\Lambda$ CDM. From the combined data analysis of Union2+BAO+CMB, we reached a similar conclusion: the difference of  $\delta\chi^2 \sim 16$  relative to the  $\Lambda$ CDM. The reason for this incompatibility is that the SN Ia data favor the large values of  $\Omega_m^{(0)}$  ( $\gtrsim 0.32$ ), whereas the CMB and BAO data constrain smaller values of  $\Omega_m^{(0)}$  ( $\lesssim 0.27$ ).

We also studied the general solutions to Eqs. (16)-(19) for the parameters  $\alpha$  and  $\beta$  constrained by the conditions for the avoidance of ghosts and instabilities. In general the solutions that approach the tracker only at late times are favored from the combined data analysis. By choosing several fixed values of  $\Omega_K^{(0)}$ , we found that the generic solutions can be consistent with the data for the open Universe ( $\Omega_K^{(0)} > 0$ ). For example, the general solutions with  $\Omega_K^{(0)} = 0.01$  and the model parameters  $(\alpha, \beta) = (1.862, 0.607)$  give the similar value of  $\chi^2$  to that in the the  $\Lambda$ CDM. In this case the AIC statistics also have the same support for the two models. For the models with largely negative  $\Omega_K^{(0)}$  such as  $\Omega_K^{(0)} \lesssim -0.01$  the data favor considerably more the  $\Lambda$ CDM model, as the fit is particularly bad.

The BIC statistics show that the general solutions, with all 4 parameters ( $\alpha, \beta, \Omega_m^{(0)}, \Omega_K^{(0)}$ ) are varied, are not particularly favored over the  $\Lambda$ CDM model (because  $\Delta\text{BIC} \gtrsim 6$ ). This mainly comes from the statistical property that the number of model parameters is larger than those in the flat  $\Lambda$ CDM. In fact the general solutions

with a non-zero curvature can be well consistent with the combined data analysis.

It will be of interest to study the evolution of matter density perturbations to confront the Galileon cosmology with the observations of large scale structure (LSS). In particular, the presence of the field derivative couplings with  $R$  and  $G_{\nu\rho}$  in the expression of  $\mathcal{L}_4$  and  $\mathcal{L}_5$  will change the effective gravitational coupling [62]. This should modify the growth rate of matter perturbations as well as the ISW effect on large-scale CMB anisotropies. Compared to the distance measures  $\mathcal{R}$  and  $l_a$  we discussed in this paper, the ISW effect is in general not so powerful to constrain dark energy models. However, in the case where the modification of the effective gravitational coupling is significant, the ISW effect may provide a strong constraint. In addition, the LSS-ISW anticorrelation found in a similar Galileon-like model [28] can be a useful tool to constrain the parameter space  $(\alpha, \beta)$  further. We will leave this issue for a future work.

## ACKNOWLEDGEMENTS

The authors are grateful to Eiichiro Komatsu, Kazuya Koyama, Shuntaro Mizuno, Pia Mukherjee, and David Wands for useful discussions. S.N. is supported by the Niels Bohr International Academy, the Danish Research Council under FNU Grant No. 272-08-0285 and the DISCOVERY center. A.D.F. thanks Burin Gumjudpai for warm hospitality during his stay in Naresuan University. S.T. is also grateful to Savvas Nesseris, Kazuya Koyama, Burin Gumjudpai, and Jungjai Lee for warm hospitalities during his stays in the Niels Bohr Institute, the University of Portsmouth, Naresuan University, and Daejeon. The work of A.D.F. and S.T. was supported by the Grant-in-Aid for Scientific Research Fund of the JSPS Nos. 09314 and 30318802. S.T. also thanks financial support for the Grant-in-Aid for Scientific Research on Innovative Areas (No. 21111006).

- 
- [1] A. G. Riess *et al.*, *Astron. J.* **116**, 1009 (1998); *Astron. J.* **117**, 707 (1999); S. Perlmutter *et al.*, *Astrophys. J.* **517**, 565 (1999).
  - [2] D. N. Spergel *et al.*, *Astrophys. J. Suppl.* **148**, 175 (2003); D. N. Spergel *et al.* [WMAP Collaboration], *Astrophys. J. Suppl.* **170**, 377 (2007).
  - [3] D. J. Eisenstein *et al.* [SDSS Collaboration], *Astrophys. J.* **633**, 560 (2005).
  - [4] W. J. Percival *et al.*, *Mon. Not. Roy. Astron. Soc.* **401**, 2148 (2010).
  - [5] E. Komatsu *et al.*, arXiv:1001.4538 [astro-ph.CO].
  - [6] V. Sahni and A. A. Starobinsky, *Int. J. Mod. Phys. D* **9**, 373 (2000); S. M. Carroll, *Living Rev. Rel.* **4**, 1 (2001); T. Padmanabhan, *Phys. Rept.* **380**, 235 (2003); P. J. E. Peebles and B. Ratra, *Rev. Mod. Phys.* **75**, 559 (2003); E. J. Copeland, M. Sami and S. Tsujikawa, *Int. J. Mod. Phys. D* **15**, 1753 (2006); A. De Felice and S. Tsujikawa, *Living Rev. Rel.* **13**, 3 (2010); P. Brax, arXiv:0912.3610 [astro-ph.CO]; S. Tsujikawa, arXiv:1004.1493 [astro-ph.CO].
  - [7] Y. Fujii, *Phys. Rev. D* **26**, 2580 (1982); L. H. Ford, *Phys. Rev. D* **35**, 2339 (1987); C. Wetterich, *Nucl. Phys. B.* **302**, 668 (1988); B. Ratra and J. Peebles, *Phys. Rev. D* **37**, 321 (1988); R. R. Caldwell, R. Dave and P. J. Steinhardt, *Phys. Rev. Lett.* **80**, 1582 (1998); I. Zlatev, L. M. Wang and P. J. Steinhardt, *Phys. Rev. Lett.* **82**, 896 (1999).
  - [8] S. Capozziello, *Int. J. Mod. Phys. D* **11**, 483 (2002); S. Capozziello, S. Carloni and A. Troisi, *Recent Res. Dev. Astron. Astrophys.* **1**, 625 (2003); S. Capozziello,

- V. F. Cardone, S. Carloni and A. Troisi, *Int. J. Mod. Phys. D* **12**, 1969 (2003); S. M. Carroll, V. Duvvuri, M. Trodden and M. S. Turner, *Phys. Rev. D* **70**, 043528 (2004).
- [9] L. Amendola, *Phys. Rev. D* **60**, 043501 (1999); J. P. Uzan, *Phys. Rev. D* **59**, 123510 (1999); T. Chiba, *Phys. Rev. D* **60**, 083508 (1999); N. Bartolo and M. Pietroni, *Phys. Rev. D* **61**, 023518 (2000); F. Perrotta, C. Baccigalupi and S. Matarrese, *Phys. Rev. D* **61**, 023507 (2000).
- [10] G. R. Dvali, G. Gabadadze and M. Porrati, *Phys. Lett. B* **485**, 208 (2000); G. R. Dvali, G. Gabadadze and M. Porrati, *Phys. Lett. B* **485**, 208 (2000).
- [11] S. Nojiri, S. D. Odintsov and M. Sasaki, *Phys. Rev. D* **71**, 123509 (2005); S. Nojiri and S. D. Odintsov, *Phys. Lett. B* **631**, 1 (2005); G. Calcagni, S. Tsujikawa and M. Sami, *Class. Quant. Grav.* **22**, 3977 (2005); T. Koivisto and D. F. Mota, *Phys. Lett. B* **644**, 104 (2007); *Phys. Rev. D* **75**, 023518 (2007); S. Tsujikawa and M. Sami, *JCAP* **0701**, 006 (2007); A. De Felice and S. Tsujikawa, *Phys. Lett. B* **675**, 1 (2009); *Phys. Rev. D* **80**, 063516 (2009).
- [12] S. M. Carroll *et al.*, *Phys. Rev. D* **71**, 063513 (2005); I. Navarro and K. Van Acoleyen, *Phys. Lett. B* **622**, 1 (2005); *JCAP* **0603**, 008 (2006); A. De Felice and T. Suyama, *JCAP* **0906**, 034 (2009); *Phys. Rev. D* **80**, 083523 (2009); A. De Felice, J. M. Gerard and T. Suyama, *Phys. Rev. D* **82**, 063526 (2010); A. De Felice and T. Tanaka, *Prog. Theor. Phys.* **124**, 503 (2010).
- [13] C. M. Will, *Living Rev. Rel.* **4**, 4 (2001); *Living Rev. Rel.* **9**, 3 (2005); B. Bertotti, L. Iess and P. Tortora, *Nature* **425**, 374 (2003).
- [14] A. De Felice, M. Hindmarsh and M. Trodden, *JCAP* **0608**, 005 (2006); G. Calcagni, B. de Carlos and A. De Felice, *Nucl. Phys. B* **752**, 404 (2006).
- [15] M. A. Luty, M. Porrati and R. Rattazzi, *JHEP* **0309**, 029 (2003); A. Nicolis and R. Rattazzi, *JHEP* **0406**, 059 (2004); K. Koyama and R. Maartens, *JCAP* **0601**, 016 (2006); D. Gorbunov, K. Koyama and S. Sibiryakov, *Phys. Rev. D* **73**, 044016 (2006).
- [16] M. Fairbairn and A. Goobar, *Phys. Lett. B* **642**, 432 (2006); R. Maartens and E. Majerotto, *Phys. Rev. D* **74**, 023004 (2006); U. Alam and V. Sahni, *Phys. Rev. D* **73**, 084024 (2006); Y. S. Song, I. Sawicki and W. Hu, *Phys. Rev. D* **75**, 064003 (2007); J. Q. Xia, *Phys. Rev. D* **79**, 103527 (2009).
- [17] B. Li, J. D. Barrow and D. F. Mota, *Phys. Rev. D* **76**, 044027 (2007); A. De Felice, D. F. Mota and S. Tsujikawa, *Phys. Rev. D* **81**, 023532 (2010).
- [18] L. Amendola, R. Gannouji, D. Polarski and S. Tsujikawa, *Phys. Rev. D* **75**, 083504 (2007); B. Li and J. D. Barrow, *Phys. Rev. D* **75**, 084010 (2007); L. Amendola and S. Tsujikawa, *Phys. Lett. B* **660**, 125 (2008); W. Hu and I. Sawicki, *Phys. Rev. D* **76**, 064004 (2007); A. A. Starobinsky, *JETP Lett.* **86**, 157 (2007); S. A. Appleby and R. A. Battye, *Phys. Lett. B* **654**, 7 (2007); S. Tsujikawa, *Phys. Rev. D* **77**, 023507 (2008); S. Tsujikawa *et al.*, *Phys. Rev. D* **77**, 103009 (2008); E. V. Linder, *Phys. Rev. D* **80**, 123528 (2009).
- [19] C. Deffayet, G. R. Dvali, G. Gabadadze and A. I. Vainshtein, *Phys. Rev. D* **65**, 044026 (2002); M. Porrati, *Phys. Lett. B* **534**, 209 (2002).
- [20] A. I. Vainshtein, *Phys. Lett. B* **39**, 393 (1972).
- [21] A. Nicolis, R. Rattazzi and E. Trincherini, *Phys. Rev. D* **79**, 064036 (2009).
- [22] C. Deffayet, G. Esposito-Farese and A. Vikman, *Phys. Rev. D* **79**, 084003 (2009); C. Deffayet, S. Deser and G. Esposito-Farese, *Phys. Rev. D* **80**, 064015 (2009).
- [23] A. De Felice and S. Tsujikawa, *Phys. Rev. Lett.* **105**, 111301 (2010).
- [24] A. De Felice and S. Tsujikawa, arXiv:1008.4236 [hep-th].
- [25] N. Chow and J. Khoury, *Phys. Rev. D* **80**, 024037 (2009).
- [26] F. P. Silva and K. Koyama, *Phys. Rev. D* **80**, 121301 (2009).
- [27] T. Kobayashi, H. Tashiro and D. Suzuki, *Phys. Rev. D* **81**, 063513 (2010).
- [28] T. Kobayashi, *Phys. Rev. D* **81**, 103533 (2010).
- [29] C. de Rham and A. J. Tolley, *JCAP* **1005**, 015 (2010).
- [30] R. Gannouji and M. Sami, *Phys. Rev. D* **82**, 024011 (2010).
- [31] A. De Felice and S. Tsujikawa, *JCAP* **1007**, 024 (2010).
- [32] A. De Felice, S. Mukohyama and S. Tsujikawa, *Phys. Rev. D* **82**, 023524 (2010).
- [33] P. Creminelli, A. Nicolis and E. Trincherini, arXiv:1007.0027 [hep-th].
- [34] A. Padilla, P. M. Saffin and S. Y. Zhou, arXiv:1007.5424 [hep-th].
- [35] C. Deffayet, S. Deser and G. Esposito-Farese, arXiv:1007.5278 [gr-qc].
- [36] C. Deffayet, O. Pujolas, I. Sawicki and A. Vikman, arXiv:1008.0048 [hep-th].
- [37] T. Kobayashi, M. Yamaguchi and J. Yokoyama, arXiv:1008.0603 [hep-th].
- [38] K. Hinterbichler, M. Trodden and D. Wesley, arXiv:1008.1305 [hep-th].
- [39] A. Ali, R. Gannouji and M. Sami, arXiv:1008.1588 [astro-ph.CO].
- [40] M. Andrews, K. Hinterbichler, J. Khoury and M. Trodden, arXiv:1008.4128 [hep-th].
- [41] G. L. Goon, K. Hinterbichler and M. Trodden, arXiv:1008.4580 [hep-th].
- [42] S. Mizuno and K. Koyama, arXiv:1009.0677 [hep-th].
- [43] C. Burrage, C. de Rham, D. Seery and A. J. Tolley, arXiv:1009.2497 [hep-th].
- [44] E. Babichev, arXiv:1009.2921 [hep-th].
- [45] D. F. Mota, M. Sandstad and T. Zlosnik, arXiv:1009.6151 [astro-ph.CO].
- [46] Y. Wang and P. Mukherjee, *Phys. Rev. D* **76**, 103533 (2007).
- [47] H. Li, J. Q. Xia, G. B. Zhao, Z. H. Fan and X. Zhang, *Astrophys. J.* **683**, L1 (2008).
- [48] R. Lazkoz, S. Nesseris and L. Perivolaropoulos, *JCAP* **0807**, 012 (2008).
- [49] J. C. B. Sanchez, S. Nesseris and L. Perivolaropoulos, *JCAP* **0911**, 029 (2009).
- [50] J. R. Bond, G. Efstathiou and M. Tegmark, *Mon. Not. Roy. Astron. Soc.* **291**, L33 (1997).
- [51] L. Amendola and S. Tsujikawa, “*Dark energy—theory and observations*”, Cambridge University Press (2010).
- [52] W. Hu and N. Sugiyama, *Astrophys. J.* **471**, 542 (1996).
- [53] E. Komatsu *et al.* [WMAP Collaboration], *Astrophys. J. Suppl.* **180**, 330 (2009).
- [54] D. J. Eisenstein and W. Hu, *Astrophys. J.* **496**, 605 (1998).
- [55] M. Hicken *et al.*, *Astrophys. J.* **700**, 1097 (2009).
- [56] R. Amanullah *et al.*, *Astrophys. J.* **716**, 712 (2010).
- [57] S. Nesseris and L. Perivolaropoulos, *Phys. Rev. D* **70**, 043531 (2004).
- [58] S. Nesseris and L. Perivolaropoulos, *Phys. Rev. D* **72**,

- 123519 (2005).
- [59] S. Nesseris and L. Perivolaropoulos, *JCAP* **0701**, 018 (2007).
- [60] A. R. Liddle, *Mon. Not. Roy. Astron. Soc.* **351**, L49 (2004).
- [61] M. Biesiada, *JCAP* **0702**, 003 (2007).
- [62] A. De Felice, R. Kase and S. Tsujikawa, arXiv:1011.6132 [astro-ph.CO].